Available online at www.sciencedirect.com
ScienceDirect
Ceramics International 35 (2009) 2261–2270
CERAMICS INTERNATIONAL
www.elsevier.com/locate/ceramint

Preparation and characterization of TiO_2, ZnO, and TiO_2/ZnO nanofilms via sol–gel process

Jintao Tian *, Lijuan Chen, Jinhui Dai, Xin Wang, Yansheng Yin, Pingwei Wu

Institute of Materials Science and Engineering, Ocean University of China, Songling Road 238, Qingdao, Shandong 266100, PR China

Received 13 October 2008; received in revised form 29 October 2008; accepted 29 December 2008
Available online 22 January 2009

Abstract

The preparation of the TiO_2, ZnO, and TiO_2/ZnO nanofilms was conducted on glass via sol–gel process. The prepared film was detailedly characterized by means of OM, SEM, XRD, and EDS. The results showed that the obtained pure TiO_2 was composed of nanoparticles. For pure ZnO it consisted of nanoparticles and large agglomerates. Both the microstructural morphology and the crystallization of the prepared TiO_2/ZnO composite film were strongly related to the Ti/Zn ratio in the film. With a Ti/Zn ratio less than 1/1, the composite film was absence of cracks. Poor crystallization was definitely observed for the composite film with Ti/Zn ratio of 3/1 and 1/1. The EDS analysis revealed homogeneous distribution of Ti and Zn elements in the film.

Keywords: Thin film; Sol–gel growth; Microstructure; Crystallization

1. Introduction

In recent years, semiconductor photocatalysis is becoming more and more attractive due to its great potential to solve environmental problems [1,2]. Titanium dioxide (TiO_2) was one of the most important semiconductors with high photocatalytic activity, being non-toxic, stable in aqueous solution, and relatively inexpensive. The excellent photocatalytic property of TiO_2 is due to its wide band gap and long lifetime of photogenerated holes and electrons [3]. The material, however, presents two main drawbacks during the photocatalytic process: (i) the low use of solar spectrum and (ii) the relatively high electron–hole recombination rate. One of efforts to overcome these problems is to dope TiO_2 with other material [3,4]. As another well-known photocatalyst, the zinc oxide (ZnO) material has received much attention with respect to the degradations of various environmental pollutants [5]. In fact, higher photocatalytic efficiency, compared to TiO_2, has been reported for ZnO [6–8]. Besides, the band gap energy of ZnO was similar to that of TiO_2 (approximately 3.2 eV) [9–11]. Thus, it is possible to enhance the activity of TiO_2 photocatalyst by means of ZnO doping. Up to now, some efforts have been done to modify TiO_2 by means of ZnO doping. The physical, chemical, and photochemical properties of the formed TiO_2/ZnO composites were mainly dependent on the manufacturing method. For instance, Aal et al. have synthesized TiO_2/ZnO nanopowders by hydrothermal method [1]. Zhang et al. prepared Zn-doped TiO_2 film by means of pulsed DC reactive magnetron sputtering method using Ti and Zn mixed target [12]. Kim et al. produced

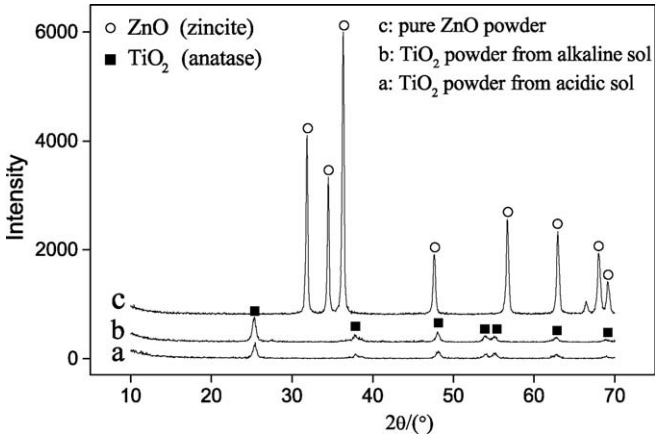

Fig. 1. XRD patterns of the TiO_2 and ZnO powders from heat treatment of TiO_2 and ZnO gel at 500 °C for 2 h.

* Corresponding author. Tel.: +86 532 66781690; fax: +86 532 66781320.
E-mail address: jttian@ouc.edu.cn (J. Tian).

0272-8842/$34.00
doi:10.1016/j.ceramint.2008.12.010

ZnO coated TiO_2 nanoparticles for use in flexible dye-sensitized solar cells [13]. Contrary to these materials, the TiO_2/ZnO nanocomposite film via sol–gel process has advantages of higher surface activity due to the nanoparticles, being not conglomerated and easily reclaimed after reaction. Moreover, the sol–gel process for nanofilm preparation, compared to other methods, has notable advantages such as high purity, good uniformity of the film microstructure, low-temperature synthesis, and easily controlled reaction condition [14,15].

In this paper we presented a detailed investigation on the TiO_2/ZnO nanocomposite film. Prior to dealing with the TiO_2/ZnO nanocomposite film, the substantial investigations

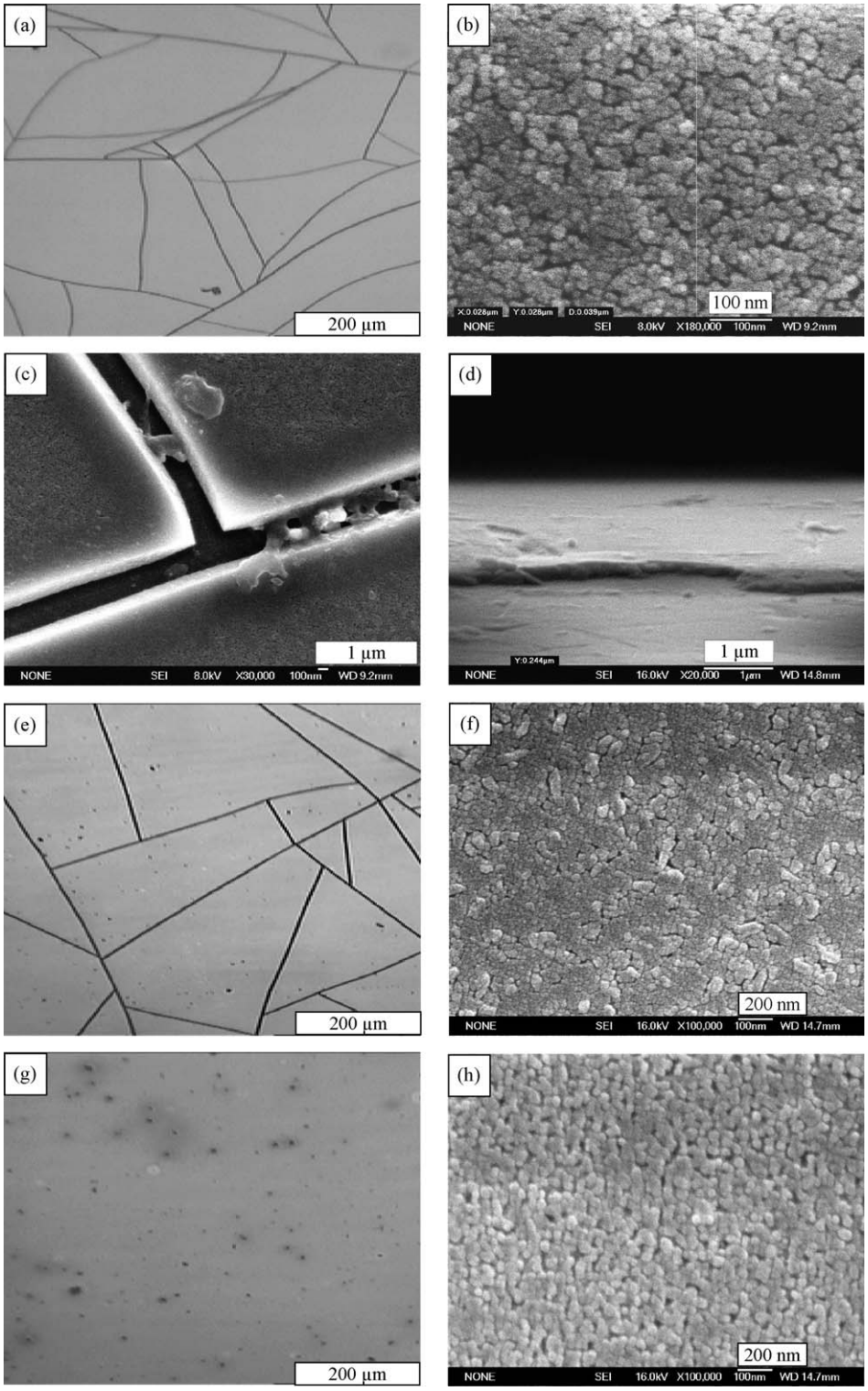

Fig. 2. Optical (a, e, and g) and SEM (b–d, f, and h) morphologies of the TiO_2 nanofilm (a–f) and the ZnO nanofilm (g and h) prepared via sol–gel process. The nanofilm in (a–d) was from acidic sol while in (e–h) they were from alkaline sol.

on the TiO_2 and ZnO nanofilms were quite essential. The preparation of the TiO_2, ZnO, and TiO_2/ZnO nanofilms were achieved via sol–gel process using glass as substrate. The as-prepared nanofilms after heat treatment were characterized using OM, SEM, EDS, and XRD methods.

2. Experimental procedure

In the present study the TiO_2, ZnO, and TiO_2/ZnO nanofilms were prepared via sol–gel process using glass as substrate. The tetrabutyl titanate (Aldrich, 99.99%, TBT) was used as a precursor and the TiO_2 sol was prepared at room temperature as follows. Firstly the TBT was dissolved in ethanol and stirred for half an hour to get a precursor solution. A mixture of distilled water, glacial acetic acid, and ethanol was then dropped into the precursor solution at a speed of one drop per second under a strong stirring. After that, the solution was continuously stirred for 1 h to achieve a yellow transparent sol. The sol was then aged for a period of time. Here glacial acetic acid was used as an inhibitor to slow down the TBT fast hydrolysis. In this case, the pH value of the system was determined to be ~5 and the obtained sol was hereafter referred to be as acidic sol. On the other hand, another inhibitor of diethanolamine (Aldrich, 99.99%, DEA) was used and the pH value of the system was determined to be ~10. The prepared TiO_2 sol in this case was referred to be as alkaline sol.

The preparation of TiO_2/ZnO sol could be achieved via directly mixing of the acidic TiO_2 sol and the ZnO sol. The ZnO sol was prepared as follows. Firstly the zinc acetate (Aldrich, 99.99%) was dissolved in ethanol and stirred for 5 min at 70 °C in water bath to get a precursor solution. A mixture of distilled water, diethanolamine, and ethanol was then dropped into the precursor solution at a speed of one drop per second under a strong stirring. After that, the solution was continuously stirred for 2 h to achieve a transparent alkaline ZnO sol. The prepared ZnO sol was then directly incorporated into the TiO_2 alkaline sol to get TiO_2/ZnO sol. The as-prepared sol was hereafter referred to be as directly mixing TiO_2/ZnO sol.

The preparation of TiO_2/ZnO sol could also be achieved via in situ mixing of Ti and Zn. In this case the TBT was dissolved in ethanol and stirred for 10 min at 70 °C in water bath. The zinc acetate was then added to get a precursor solution containing both Ti and Zn. A mixture of distilled water, diethanolamine, and ethanol was dropped into the solution at a speed of one drop per second under a strong stirring. After that, the solution was continuously stirred for 2 h to achieve a transparent TiO_2/ZnO sol. The as-prepared sol in such a case was hereafter referred to be as in situ mixing TiO_2/ZnO sol.

The preparation of the TiO_2, ZnO, and TiO_2/ZnO nanofilms was conducted via sol–gel process using glass as substrate (a softening temperature of 600–650 °C for this glass from the supplier). Prior to the coating process, the glass was washed with water, ultrasonically cleaned in ethanol for 20 min, and in acetone for 20 min, respectively. The prepared TiO_2, ZnO, and TiO_2/ZnO sol was coated onto the substrate surface via dip-coating method at a withdrawal speed of 2 mm/s. After natural drying in air, the coating operation was repeated again. The

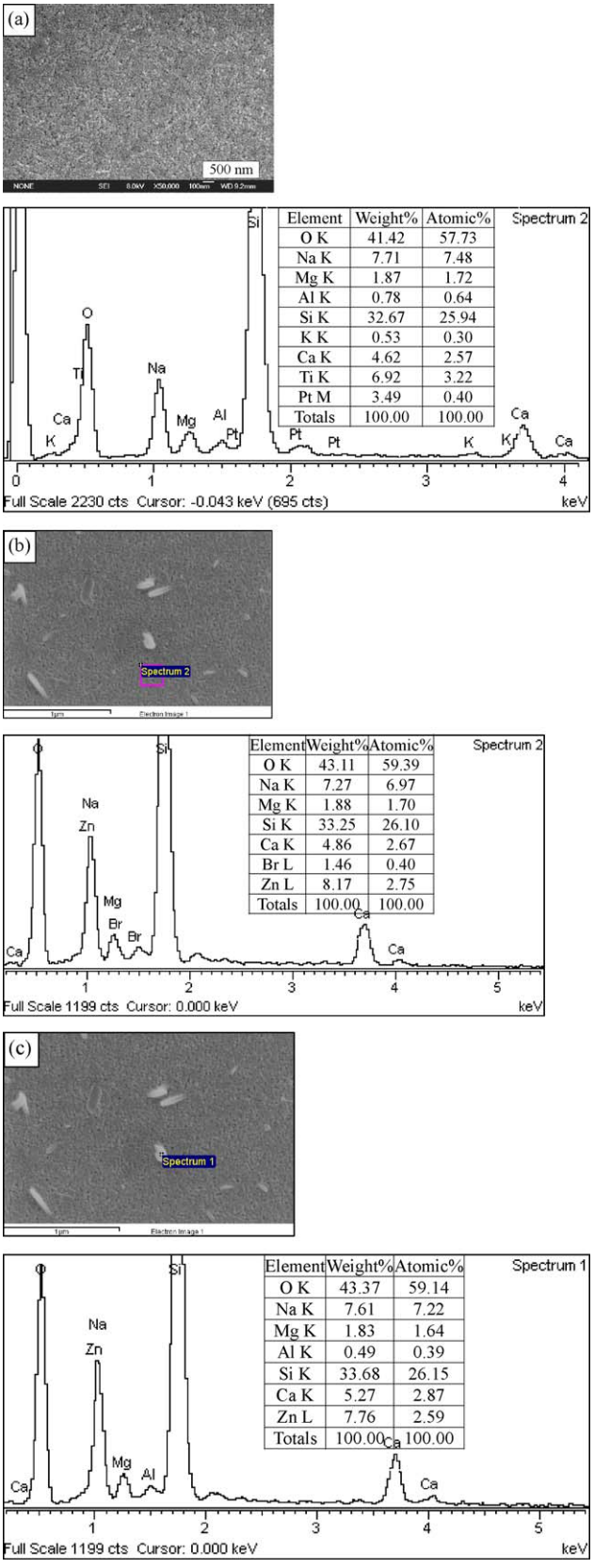

Fig. 3. EDS analysis of the TiO_2 nanofilm (a) and the ZnO nanofilm (b and c) prepared via sol–gel process.

coated specimen was then heat treated at 100 °C for 1 h and then at 500 °C for 2 h. The temperature increase during this process was kept at a speed of 1 °C/min. After heat treatment, the specimen was naturally cooled.

The as-prepared TiO_2, ZnO, and TiO_2/ZnO nanofilm was characterized as below. The crystalline phase of the film was identified through X-ray diffraction (XRD) method. The surface morphology of the film was observed using optical microscope (OM) and scanning electron microscopy (SEM). The elemental analysis of the film was performed using energy dispersive spectroscopy (EDS).

3. Results and discussion

3.1. The TiO_2 and ZnO nanofilms

The TiO_2 nanofilm was prepared on glass via sol–gel process. In order to identify the phase composition of the film, the XRD measurement was conducted on the coated substrate glass. There have no peaks appeared in the XRD patterns, indicating an amorphous state of the sample. Similar result was obtained for the uncoated substrate glass. In order to confirm whether a proper heating process for the film crystallization was applied or not, the TiO_2 sol was gelled and heat treated to be powders under the same heating process. The XRD measurement was performed on the powders. The results were shown in Fig. 1. With the heat treatment of 500 °C for 2 h, the crystallized TiO_2 of anatase was obtained. This indicated that the amorphous TiO_2 could be well crystallized under such heating process. The crystalline TiO_2 film was presumably too thin to be detected out during the XRD measurement and therefore was absent in the XRD patterns. Similar result was obtained for the ZnO nanofilm. The crystalline ZnO of zincite was formed. One interesting point in Fig. 1 was that the TiO_2 powder prepared from alkaline sol shows diffraction intensity peaks evidently higher than those of the TiO_2 powder from acidic sol, indicating better crystallization of the film from alkaline sol than the film from acidic sol. Thus, the crystallization behavior of the pure TiO_2 film was clearly affected by the addition of inhibitor.

The substrate glass after the film coating was transparent. The optical and SEM observations of the TiO_2 and ZnO nanofilm were performed and the results were shown in Fig. 2. Both the TiO_2 films prepared from the acidic sol and the alkaline sol showed many cracks (Fig. 2a and e). These cracks were from the removal of residual hydroxyl and organic groups during the heat treatment process. A typical crack morphology was shown in Fig. 2c, giving a crack width of ~300 nm. The film thickness was estimated to be ~250 nm (Fig. 2d). Such estimation was in good agreement with the results from XRD measurements above, where the film was presumed to be rather thin. Both the TiO_2 films prepared from the acidic sol and the alkaline sol were composed of nanoparticles. The particle morphologies of the two films, however, were noticeably different (Fig. 2b and f). The TiO_2 nanoparticles from the acidic sol exhibited a narrow particle size distribution of ~15 nm to ~30 nm. In the case of the TiO_2 film from the alkaline sol, the particle distribution was in a broad range of ~10 nm to ~80 nm. The particle morphology of the TiO_2 nanofilm was therefore remarkably affected by the addition of the inhibitor.

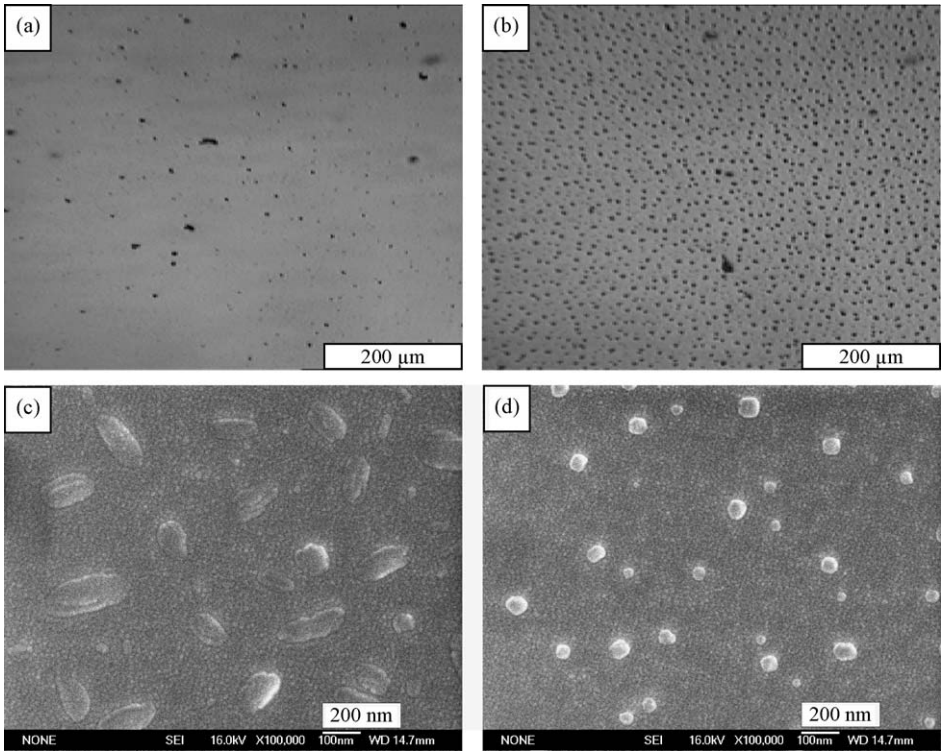

Fig. 4. Optical (a and b) and SEM (c and d) morphologies of the TiO_2/ZnO nanocomposite film prepared via sol–gel process from in situ mixing TiO_2/ZnO sol. Before film coating, the sol was aged for 28 h (a and c) and 96 h (b and d), respectively. The atomic ratio of Ti to Zn here was kept to be 1/1.

Besides the TiO_2 nanofilm, the ZnO nanofilm was also presented in this figure. The surface morphology of the ZnO film was much different from that of the TiO_2 film. The as-prepared ZnO film was composed of nanoparticles. No crack was found present. Some large agglomerates were dispersed homogeneously in the film. The ZnO nanoparticles exhibited a narrow particle size distribution of ~20 nm to ~40 nm (Fig. 2h).

In order to clarify the element composition of the prepared film, the EDS analysis was conducted on the surface of the TiO_2 and ZnO nanofilms during SEM observations. The results were shown in Fig. 3. Elements of oxygen (O), silicon (Si), sodium (Na), calcium (Ca), etc. were detected to be present on the surface of the specimen (Fig. 3a–c). These elements were from the substrate glass. This indicated that the prepared film was rather thin. The platinum (Pt) was from the platinum coating for electron conductivity. The presence of titanium (Ti) indicated that the TiO_2 film has been successfully formed on the substrate (Fig. 3a). The zinc (Zn) was also found present in the ZnO nanofilm (Fig. 3b). The EDS results for the large agglomerates in the ZnO film indicated that these agglomerates were containing Zn element (Fig. 3c). They were large particles of ZnO.

3.2. The TiO_2/ZnO nanocomposite film from in situ mixing TiO_2/ZnO sol

The TiO_2/ZnO nanocomposite film was firstly prepared via sol–gel process from in situ mixing TiO_2/ZnO sol. The optical and SEM observations were performed and the results were shown in Fig. 4. Here the effect of aging time of the TiO_2/ZnO sol on the film microstructures was studied. The aging time of

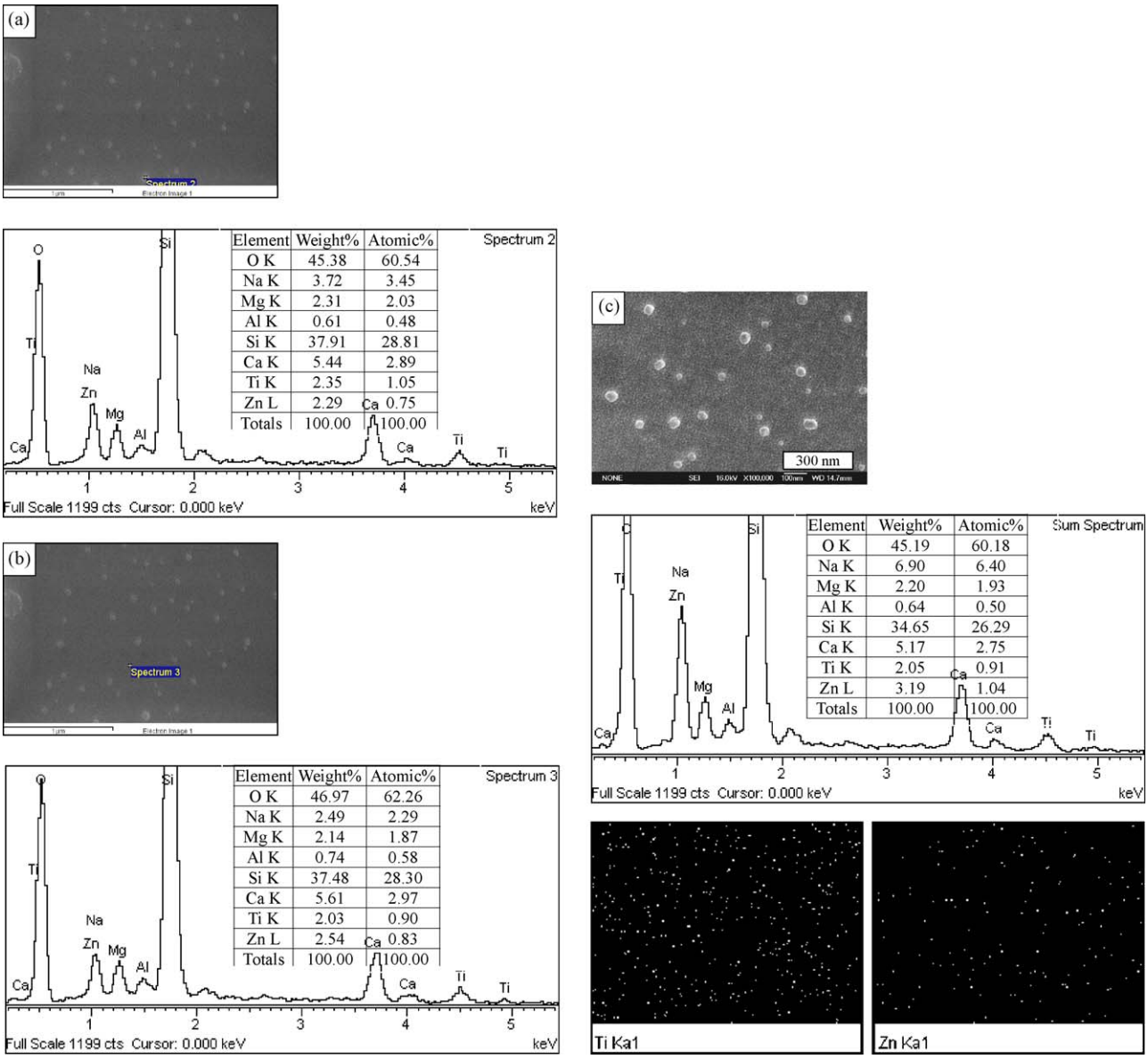

Fig. 5. EDS analysis of the TiO_2/ZnO nanocomposite film prepared via sol–gel process from in situ mixing TiO_2/ZnO sol. Before film coating, the sol was aged for 96 h and the atomic ratio of Ti to Zn was kept to be 1/1.

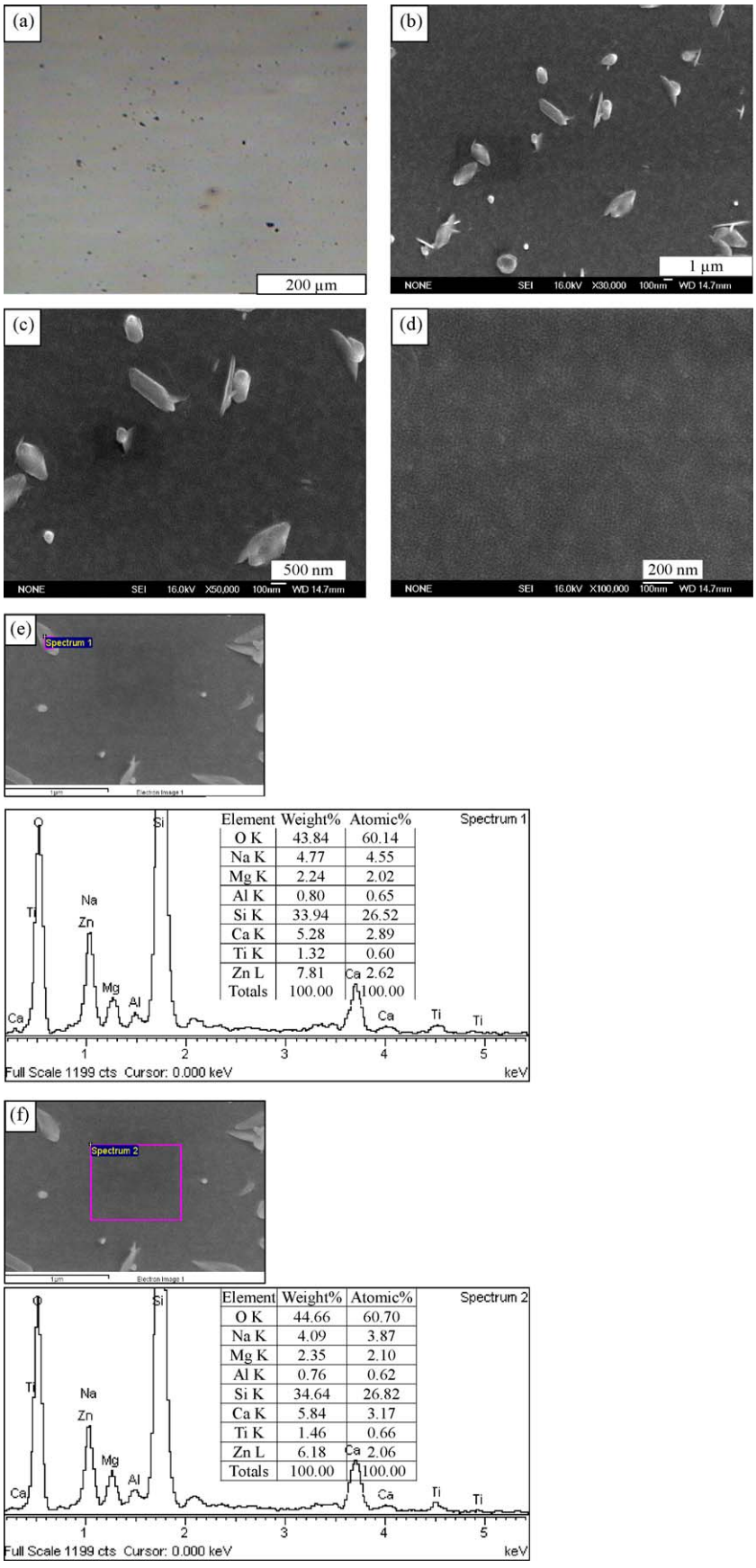

Fig. 6. Optical (a) and SEM (b–d) morphologies of the TiO_2/ZnO nanocomposite film prepared via sol–gel process from directly mixing TiO_2/ZnO sol. The EDS analysis of the film was also incorporated in this figure (e and f). The atomic ratio of Ti to Zn was kept to be 1/3.

the sol was 24 h (Fig. 4a and c) and 96 h (Fig. 4b and d). The atomic ratio of Ti to Zn was kept to be 1/1 in the two cases. From Fig. 4a and c we could find that large agglomerates were dispersed homogenously in the film. Most of these agglomerates were in a size of ∼100 nm. After another three days aging (ageing time of totally 96 h), the agglomerates grew up to be in microscale (Fig. 4b). Further SEM observations at high magnification indicated that besides these microscale agglomerates, some small agglomerates with a size of ∼50 nm were present in the film (Fig. 4d). The as-prepared TiO_2/ZnO film was composed of large agglomerates and nanoparticles that were in a narrow size distribution of ∼5 nm to ∼15 nm. There has no crack in the composite film.

The EDS analysis of the TiO_2/ZnO nanocomposite film was performed and the results were given in Fig. 5. Again, the elements of O, Si, Ca, Na, etc. were from the substrate glass. For the EDS analysis on the large agglomerates, elements of Ti and Zn were detected to be present, indicating the agglomerates containing elements of both Ti and Zn (Fig. 5a). The agglomerates were therefore supposed to be TiO_2/ZnO particles. The atomic ratio of Ti to Zn was close to 1/1. Similar results were obtained for the EDS analysis on the nanoparticle area (Fig. 5b). The element map scanning during the EDS analysis was conducted and the results were given in Fig. 5c. The two elements of Ti and Zn were homogenous dispersed in the whole composite film.

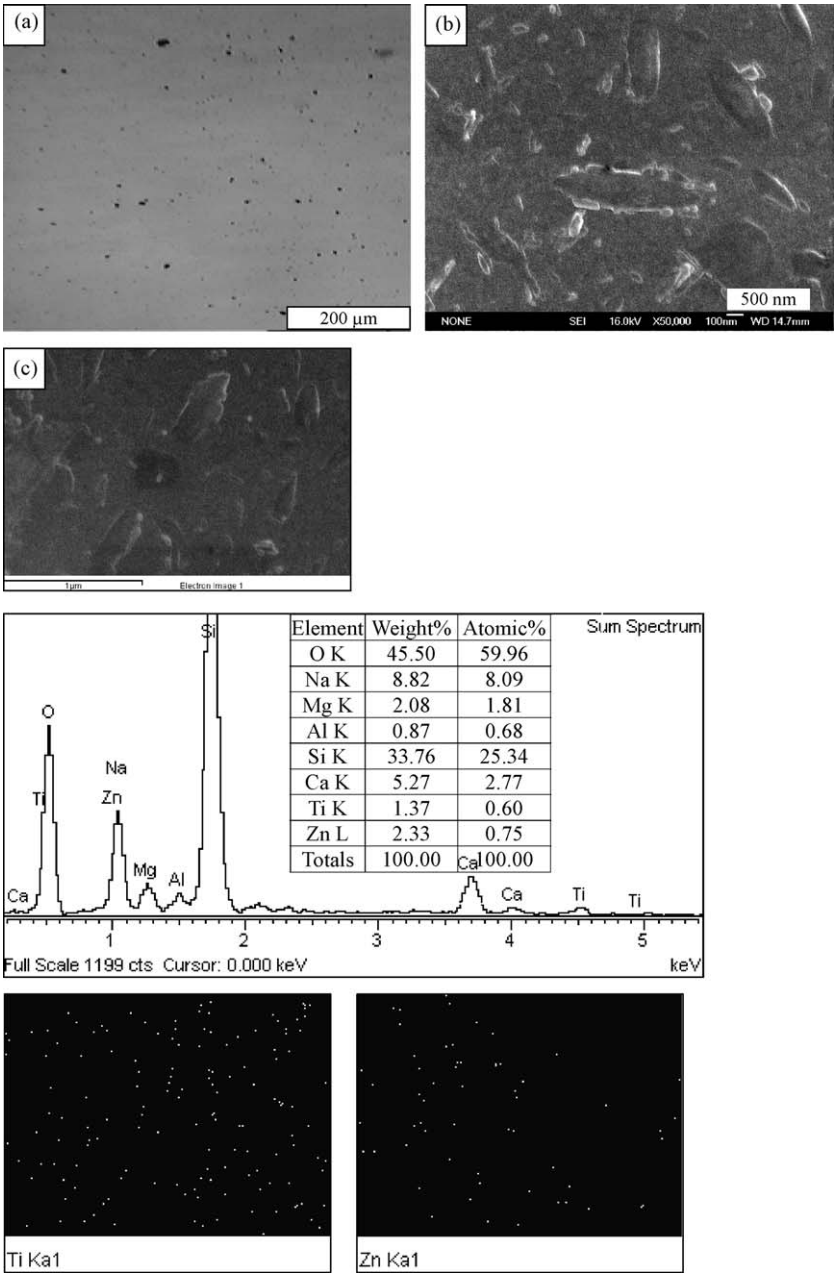

Fig. 7. Optical (a) and SEM (b) morphologies of the TiO_2/ZnO nanocomposite film prepared via sol–gel process from directly mixing TiO_2/ZnO sol. The EDS analysis of the film was also incorporated in this figure (c). The atomic ratio of Ti to Zn was kept to be 1/1.

3.3. The TiO_2/ZnO nanocomposite film from directly mixing TiO_2/ZnO sol

The TiO_2/ZnO nanocomposite film was also prepared via sol–gel process from directly mixing TiO_2/ZnO sol. In this case the atomic ratio of Ti to Zn was selected to be 1/3, 1/1, and 3/1. The optical and SEM observations of the microstructures of the composite film were conducted. The results for the film with the Ti/Zn ratio of 1/3 were shown in Fig. 6. As seen from Fig. 6, the as-prepared nanocomposite film was composed of large agglomerates and nanoparticles (Fig. 6a). The agglomerates were in a size range of ∼100 nm to ∼500 nm (Fig. 6b and c) while the nanoparticles were in a range of ∼5 nm to ∼15 nm (Fig. 6d). The EDS analysis showed that the Ti and Zn elements were present in the agglomerates (Fig. 6e). This indicated that the agglomerates were of TiO_2/ZnO particles, though the estimated Ti/Zn ratio in this figure was traceably lower than 1/3. The Ti and Zn elements were present on the nanoparticle area. The estimated Ti/Zn ratio was of accurately 1/3 (Fig. 6f). No crack was observed in the composite film.

The optical and SEM results for the composite film with the Ti/Zn ratio of 1/1 were shown in Fig. 7. The as-prepared nanocomposite film was composed of large agglomerates and nanoparticles, similar to that of the film with the Ti/Zn ratio of 1/3 (see Figs. 6a and 7a). The detailed morphologies of the film at high magnification, however, revealed remarkable microstructural difference between the two films. With a Ti/Zn ratio of 1/1, the large agglomerates were imbedded in the film while in the case of the Ti/Zn ratio of 1/3 the agglomerates were separately dispersed on the surface of the film (see Figs. 6b and 7b). The EDS analysis showed that the composite film was composed of Ti and Zn elements. The Ti/Zn ratio was of approximately 1/1. The elements of both Ti and Zn were homogeneously distributed in the film.

In the case of the Ti/Zn ratio of 3/1, the film was composed of small agglomerates and nanoparticles with a size range of ∼5 nm to ∼15 nm (Fig. 8a and b). One interesting point was that in Fig. 8a there have cracks appeared in the film. This was contrary to those of the TiO_2/ZnO composite films with the Ti/ZnO ratios of 1/1 and 1/3 (see Figs. 4a, 6a, and 7a). Note that for the TiO_2 nanofilm the cracks were present in the film (Fig. 2a) while in the case of the ZnO film they were absent (Fig. 2g). This indicated that the crack formation was strongly related to the Ti/Zn ratio of the composite film. The EDS analysis revealed the presence of the Ti and Zn elements in the composite film.

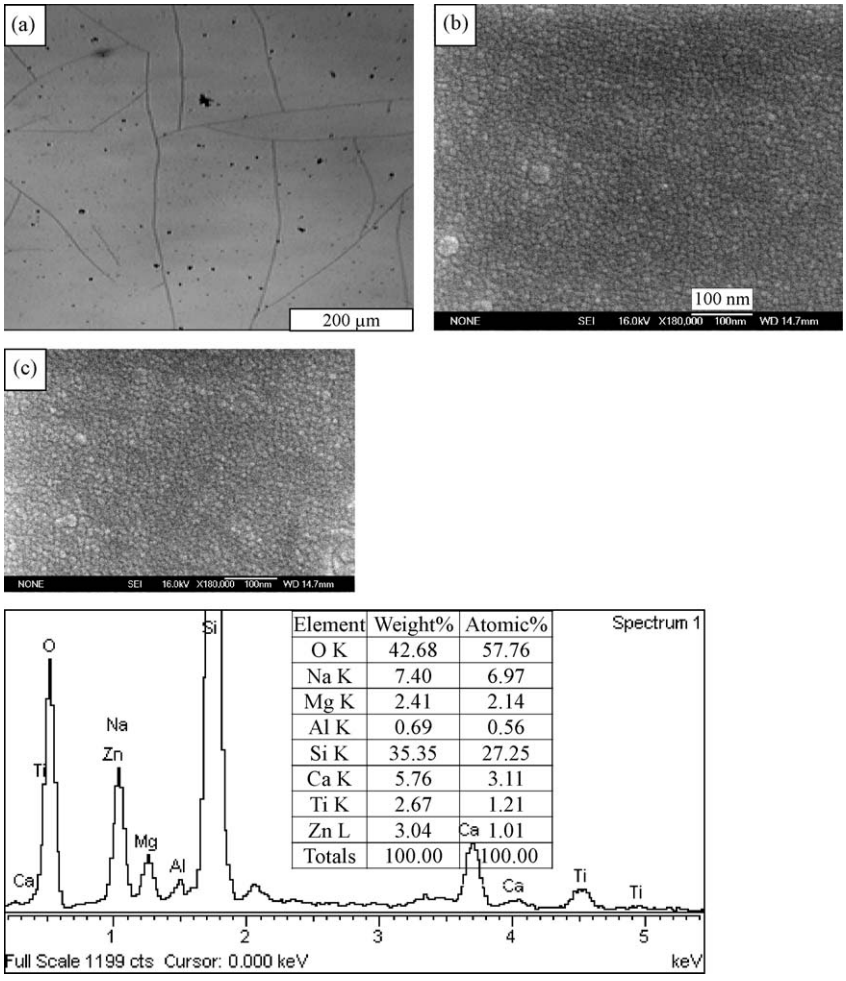

Fig. 8. Optical (a) and SEM (b) morphologies of the TiO_2/ZnO nanofilm prepared via sol–gel process from directly mixing TiO_2/ZnO sol. The EDS analysis of the film was also incorporated in this figure (c). The atomic ratio of Ti to Zn was kept to be 3/1.

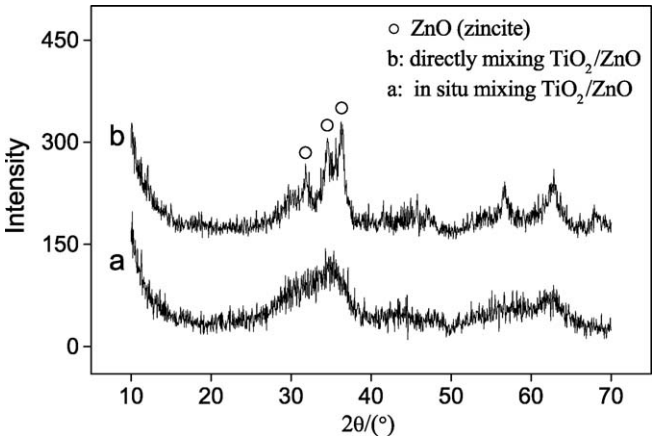

Fig. 9. XRD patterns of the TiO_2/ZnO composite. The atomic ratio of Ti to Zn was kept to be 1/1.

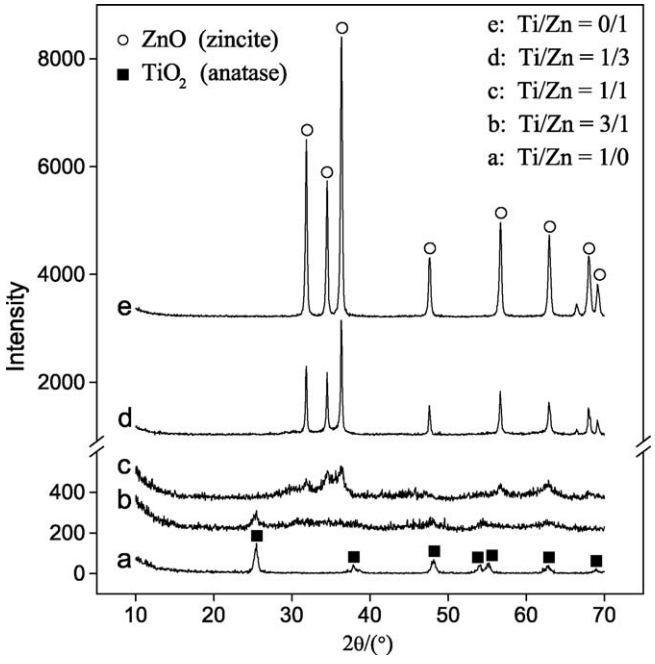

Fig. 10. XRD patterns of the TiO_2/ZnO composite from directly mixing TiO_2/ZnO sol. For Ti/Zn ratio of 1/0, the acidic TiO_2 sol was used.

3.4. The crystallization of the TiO_2/ZnO nanocomposite film

As demonstrated in Section 3.1, the crystalline phase was not able to be detected out from the thin film. The heat treated powder was therefore used during the XRD measurement. Here we used the same process to investigate the crystallization of the TiO_2/ZnO nanocomposite film. Firstly the two TiO_2/ZnO composite powders were prepared from in situ mixing sol and directly mixing sol, respectively. The XRD measurements were conducted on the two powders and the results were shown in Fig. 9. As seen from Fig. 9, the powder from directly mixing TiO_2/ZnO sol showed better crystallization than that from in situ mixing sol. Such result could be well understood by considering the particle formation and crystallization during the sol preparation process. For directly mixing sol, the small TiO_2 and ZnO particles were formed before the sol mixing. It was supposed that the mixing process would lead to less effect on the particle crystallization. In the case of in situ mixing sol, it was presumed that the added ions of Ti and Zn affected each other and therefore did not favor to the particle formation and crystallization.

The detailed investigations of crystallization on the TiO_2/ZnO composite were shown in Fig. 10. The TiO_2 particles were crystallized well (Fig. 10a). As the ion of Zn was incorporated, the resulted particles were almost amorphous. Only traceable TiO_2 peak of anatase was appeared in the XRD patterns (Fig. 10b). With a Ti/Zn ratio of 1/1 the TiO_2 peak was absent and the ZnO peak of zincite was observed (Fig. 10c). The low intensity peak in this case indicated that the composite was rather amorphous. With a Ti/Zn ratio of 1/3 the composite was well crystallized (Fig. 10d). In the case of pure ZnO the film was completely crystallized to be zincite (Fig. 10e). These results indicated again that the crystallization of the TiO_2/ZnO composite was strongly related to the addition of Zn ion and its amount.

4. Conclusions

The preparation of the TiO_2, ZnO, and TiO_2/ZnO nanofilms was conducted via sol–gel process using glass as substrate. The prepared film was detailedly characterized by means of OM, SEM, XRD, and EDS. The results indicated that the pure TiO_2 nanofilm was composed of nanoparticles. Many cracks were present on the surface of the TiO_2 film. In the case of the ZnO film no crack was observed. Some large agglomerates were dispersed homogeneously in the ZnO film. The TiO_2/ZnO nanocomposite film could be successfully prepared via sol–gel process from both in situ mixing TiO_2/ZnO sol and directly mixing TiO_2/ZnO sol. The microstructural morphology and the crystallization of the TiO_2/ZnO nanocomposite film were strongly related to the Ti/Zn ratio. With a Ti/Zn ratio less than 1/1, no crack was observed in the composite film. Some large agglomerates were dispersed homogeneously. Poor crystallization was definitely observed for the composite film with Ti/Zn ratio of 3/1 and 1/1. The EDS analysis revealed homogeneous distribution of Ti and Zn elements in the film.

Acknowledgements

This work was financially supported by the National Natural Science Foundation of China (Grant No. 50672090) and the Nature Science Foundation of Shandong Province (Y2005F15).

References

[1] A.A. Aal, M.A. Barakat, R.M. Mohamed, Appl. Surf. Sci. 254 (2008) 4577.
[2] L. Jing, B. Xin, F. Yuan, B. Wang, K. Shi, W. Cai, H. Fu, Appl. Catal. A: Gen. 275 (2004) 49–54.
[3] X. Zhang, F. Zhang, K.Y. Chan, Mater. Chem. Phys. 97 (2006) 384.
[4] P. Pichat, Nouv. J. Chem. 11 (1987) 135.
[5] Q. Zhang, W. Fan, L. Gao, Appl. Catal. B: Environ. 76 (2007) 168–173.

[6] A.A. Khodja, T. Sehili, J.F. Pilichowski, P. Boule, J. Photochem. Photobiol. A: Chem. 141 (2001) 231–239.
[7] C. Lizama, J. Freer, J. Baeza, H.D. Mansilla, Catal. Today 76 (2002) 235–246.
[8] V. Houskova, V. Stengl, S. Bakardjieva, N. Murafa, A. Kalendova, F. Oplustil, J. Phys. Chem. Solids 68 (2007) 716–720.
[9] G. Marci, V. Augugliaro, M.J. Lopez-Munoz, C. Martin, L. Palmisano, V. Rives, Phys. Chem. B 105 (2001) 1033–1040.
[10] C.C. Hsu, N.L. Wu, J. Photochem. Photobiol. A: Chem. 172 (2005) 269–274.
[11] D.K. Zhang, Y.C. Liu, Y.L. Liu, H. Yang, Physica B 351 (2004) 178–183.
[12] W. Zhang, S. Zhu, Y. Li, F. Wang, Vacuum 82 (2008) 328–335.
[13] S. Kim, J. Yum, Y. Sung, J. Photochem. Photobiol. A: Chem. 171 (2005) 269–273.
[14] L. Hu, T. Yoko, H. Kozuka, Thin Solid Films 219 (1992) 18.
[15] P. Chrysicopoulou, D. Davazoglou, C. Trapalis, G. Kordas, Thin Solid Films 323 (1998) 188.